PV Characterization and MPPT Based on Characteristic Impedance Using Arduino Board and MATLAB Interface

Mohamed BOUSSAADA[1]*, Riadh ABDELATI[1], Hajer LAHDHIRI[2], Hedi YAHIA[1]

[1] Research Laboratory of Automatic, Electrotechnical Systems and Environment (LAS2E), National School of Engineers of Monastir (ENIM), University of Monastir, Avenue Ibn El Jazzar, 5019 Monastir, Tunisia
m_boussaada@yahoo.fr (**Corresponding author*), riaabdelati@yahoo.fr, hyahia1960@gmail.com

[2] Department of Electrical Engineering, National School of Engineers of Monastir (ENIM), University of Monastir, Avenue Ibn El Jazzar, 5019 Monastir, Tunisia
lahdhiri.hajer@gmail.com

Abstract: Photo-Voltaic (PV) panels, whose maximal point is called the Maximum Power Point (MPP), provide extracted electrical power. In order to effectively exploit the PV System (PVS), they must be operated within the limits of this point. Later, it depends on the impedance of the connected load and on the Characteristic Impedance of the PV (CIPV) panel that varies with different climatic conditions. In a well-matched system, the load impedance is close to the CIPV and it operates normally at the MPP (via direct connection). Otherwise, coupling is fairly poor. The load impedance is different from the CIPV and, therefore, it requires the inclusion of MPP Tracking (MPPT) and a DC/DC converter as an adaptive load. In this paper, a new MPPT method based on CIPV matching is proposed. The algorithm structure is simple and easy to implement. This study focuses on how the PVS, tested and evaluated under varying load and climatic conditions, operates with the proposed MPPT controller. The present approach is characterized by a stable oscillation, with a slight fluctuation around the MPP. The controller integrates a variable step-size control and provides a rapid and precise convergence to the MPP. The simulation and experimental results prove the efficiency of the proposed method.

Keywords: PVS, DC/DC boost converter, CIPV, Load impedance, MPPT, Stateflow®, PWM.

1. Introduction

Although studies and research in the field of renewable energy and energy supply networks have recorded a lot of achievements and made significant progress over the last years, scientific and engineering efforts still need to be identified in the field of energy technologies. New concepts and solutions have been introduced for electric power systems and power generation, especially through the Photo-Voltaic (PV) cells or panels in theoretical and practical ways (Chellal et al., 2021; Ibnelouad et al., 2021). Power electronics research with software tools remain among the best ways to exploit the power produced by any PV cell/ module or panel. In fact, this power is produced through sunlight converted directly by using PV cells (Kanth et al., 2015). The produced power level is influenced by sun irradiation and climatic temperature (Senthilkumar et al., 2022; Salih et al., 2016). It will move upwards on the power axis when the solar irradiation increases, and it will decrease with a rise in temperature (Haihong et al., 2016; Routray et al., 2021). Moreover, a single PV cell produces low capacity power.

Therefore, to have a high power level, a serial and/or parallel assembly of these PV cells forms a module. Then, the modules are arranged in series and/or in parallel to obtain a PV panel (Kanth et al., 2015). Nevertheless, this arrangement alone can not get the Maximum Power (MP), and it is achieved only with an optimal load (Anani & Ibrahim, 2020). In this case, the PV System (PVS) is in a matched system, the load is directly connected to the PV panel, and its impedance is close to the Characteristic Impedance of PV (CIPV) sources. Otherwise, the coupling is fairly poor, the impedance load is different from the CIPV, and the MP is not ensured, where the CIPV is the internal impedance of a PV source when these sources operate at their MP Point (MPP). Indeed, regardless of this arrangement and any climatic conditions (irradiation, temperature), a PV cell or panel has an MP capacity and any PVS device is assumed to reach that capacity (Boutabba et al., 2018). Therefore, to get and extract this power level and to achieve the efficiency of the PVS, it is necessary to follow the optimum feed point for PV panels using an MPP Tracking (MPPT) algorithm (Sruthy & Mohan, 2017). Using a DC-DC converter and the MPPT algorithm, this MP is guaranteed. The converter is controlled with a Pulse Width Modulation (PWM) signal, which is generated according to this algorithm. Different techniques are used to obtain a PWM. The analog mode is obtained by comparing a progressive linear voltage with a saw-tooth signal (Boussaada et al., 2018). The digital mode is obtained by a microcontroller (Khatib et al., 2017), DSPIC (Sruthy & Mohan, 2017; Jana et al., 2016), DSPACE (Boutabba et al., 2018), or an Arduino Uno® board.

https://doi.org/10.24846/v32i1y202309

In the specialized literature, different works using a DC-DC converter and an MPPT controller to extract the MP of a PV panel have been proposed (Sruthy & Mohan, 2017), as well as various models of PV panels and DC-DC converters that were simulated in a MATLAB/Simulink® environment. To achieve this task, a lot of MPPT techniques have been exploited. Sengar (2014) discussed the advantages and disadvantages of many of these techniques, such as the differential method, the Perturb and Observe (P&O) method, Incremental Conductance (IncCond), curve fitting, open-circuit voltage Generator PV (GPV) and short-circuit GPV. Remy et al. (2009) also discussed these later in the PVS field. They commanded a boost converter with an MPPT algorithm, and they implemented various techniques with a MATLAB code. Yadav et al. (2012) proposed a comparison between an MPPT algorithm and a DC-DC converter. They compared the two most popular algorithms of P&O and IncCond using theoretical and simulation tools. They implemented these algorithms once with a buck converter and once with a boost converter. They proved that the buck converter would give the best result and that the P&O algorithm was better than the IncCond algorithm (Abouda et al., 2013).

In this context, a new MPPT algorithm is put forward in this work. It is based on the CIPV and it can be used with a DC-DC boost converter to obtain the MP of a PV panel. A resistive load is adapted to the PV panel.

Generally, in the conventional method of the MPPT controller, PWM signals with a fixed-step duty cycle are used. Depending on the step size, a fast or a slow response is obtained with strong or weak oscillations around that point. If the step size is large, a quick response is obtained, but there will be a strong fluctuation around this point. On the other hand, if the step size is small, a weak oscillation is obtained that point, but with a slow response.

The main contribution of this paper is to find a compromise between the oscillations and the response time while tracking the MPP, based on the proposed algorithm and on how the PWM signal evolves to address these issues. In fact, the duty cycle of the PWM is calculated by MATLAB/Stateflow®. As far as known, no work has calculated before such a duty cycle using Stateflow®. Generally, a lot of researchers have worked on a variable step size (Jana et al., 2016) to adjust the duty cycle of the PWM signal. In the present work, Stateflow® is utilized to increment or decrement the duty cycle using a specific step size. The present proposal is characterized by the use of the variable step, in order to ensure the efficiency of the process (PVS). Firstly, the process starts with a large step to ensure a fast response. Secondly, when the MPP is detected, the steps take small values to have a weak oscillation. The proposed method aims to resolve any complexity in the conventional methods and to preserve its acceptable results for MPPT. Indeed, in the specialized literature, researchers have used MPPT (Fares et al., 2017) or characterization (Alshareef, 2021) where each of their implementations is independent of the other. In this study, both MPPT and the characterization with the same implementation are used, which represents the second contribution of this paper. In the PV characterization a fixed step is opted for, where the duty cycle is incremented by Stateflow®. Basically, small steps can be chosen to sweep lots of points of the I-V and P-V characteristic curves.

Furthermore, an interface is developed using an Arduino Uno® board that can communicate with a chopper utilizing MATLAB/Simulink® via the proposed algorithm, creating a PWM signal. This PWM signal can also be used to characterize the PV panel when the duty cycle is in a progressive and continuous variation between [0, 1]. Consequently, the I-V and P-V curves can be carried out. Moreover, the proposed algorithm can detect the variation in the power acquired and vary the duty cycle in order to stabilize the PVS to its optimum power. Stateflow® is used to increment or decrement the duty cycle, which is received by the Arduino board. Then a PWM signal is created, and it drives the boost converter with adapted circuits. The remainder of the paper is organized as follows. Section 2 is dedicated to a detailed description of the PVS model. In section 3, the characterization and optimization of the PV panel function are presented. Section 4 provides the experimental results that validate the theoretical analysis. Section 5 concludes this paper.

2. Description of Proposed System

Figure 1 shows the block diagram of a PVS that is proposed to extract MP. It consists of a solar panel and a boost DC-DC converter connected to a load and controlled by an Arduino Uno® board,

which communicates with an interface tool using PC software.

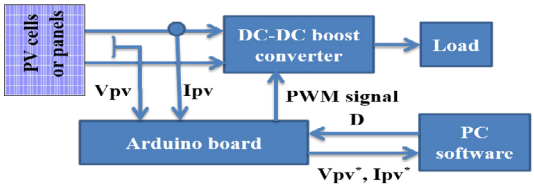

Figure 1. PVS design

In Figure 1, I_{pv} and V_{pv} are analog data received by the Arduino board, I_{pv}^{*} and V_{pv}^{*} are numerical data delivered by this board, and D is a duty cycle calculated by the PC software, where the PWM signal is delivered by this board.

2.1 PV Solar Cell Effect

Under the PV effect, a solar photon attacks a p-n semiconductor, the basic element of a solar cell, which creates an electric current I_{pv} and generates a V_{pv} potential voltage (Zhou & Macaulay, 2017), as illustrated in Figure 2.

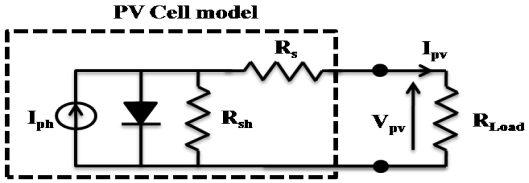

Figure 2. Electrical model of PV cell

I_{pv} and V_{pv} are in a linear relationship at the R_{Load} side. This relation is defined as follows:

$$V_{pv} = R_{Load} I_{pv} \quad (1)$$

However, they are in a non-linear relationship at the PV source side. This relation is defined as follows (Boussaada et al., 2018; Zhou & Macaulay, 2017):

$$I_{pv} = I_{ph} - I_s \left[\exp^{(V_{pv}+R_s I_{pv})/V_T} - 1 \right] - \frac{V_{pv} + R_s I_{pv}}{R_{sh}} \quad (2)$$

where $(I_{ph}, I_s, V_T, R_s, R_{sh})$ is a parameter vector of the PV panel, I_{ph} is the photocurrent, I_s is the reverse saturation current, $V_T = AKT/q$ is the thermodynamic voltage, A is the diode ideality constant, $q = 1.6*10^{(-19)\circ}C$ is the electronic charge, $K = 1.38*10^{(-23)} J/K$ is the Boltzmann constant, and T is the ambient temperature in Kelvin.

Equation (2) represents the mathematical model used to simulate any PV panel characteristics whose curves are given in Figure 3.

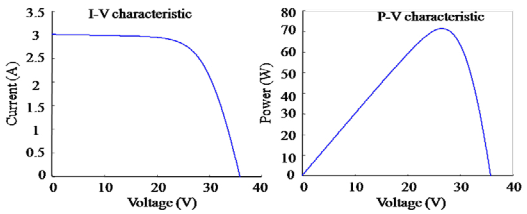

Figure 3. PV panel characteristics

Load R_{Load} consumes P_{pv} power and is expressed by:

$$P_{pv} = V_{pv} I_{pv} = R_{Load} I_{pv}^2 \quad (3)$$

This power depends on the value of the load level and on climatic conditions (irradiation, temperature) (Sruthy & Mohan, 2017; Husain et al., 2017). Any operating point is given by the intersection of the I-V characteristic of the connected load with that of the PV panel, as depicted in Figure 4.

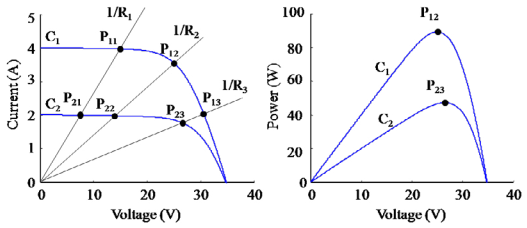

Figure 4. Power variation depending on both load and climatic conditions

In Figure 4, P_{ij} is the power level, C_i is the PV panel characteristic curves, and R_j is the load R_{Load}, with i=1, 2, and j=1, 2, 3. As a result, the MPP is P_{12} when the PV panel is characterized by C_1 and the load is R_2. It becomes P_{23} when the operating point is at C_2 and R_{23}. Else, any other combination (ij) will not succeed in obtaining the MPP. It is concluded that for any I-V characteristic, there is only one resistance value of R_{Load} which corresponds to the MPP.

2.1.1 Block Schema in MATLAB/ Simulink® of PV Panel

It is possible to simulate the PV characteristics by utilizing the mathematical model from equation (2), using MATLAB/Simulink®, as illustrated in Figure 5.

2.1.2 Simulation of PV Panel

To generate PV panel characteristics in an experimental way and/or simulation tools, different

methods are used, like the variable resistor, the capacitive load and the DC-DC converter (Boussaada et al., 2018; Khatib et al., 2017; Brito et al., 2014). In simulation techniques, as in MATLAB/Simulink®, the mathematical model from equation (2) is implemented, as depicted in Figure 5. Moreover, vector $(I_{ph}, I_s, V_T, R_s, R_{sh})$ characterizes the main parameters of the PV panel.

Current I_{pv} and voltage V_{pv} are measured in an experimental bench, and $(I_{ph}, I_s, V_T, R_s, R_{sh})$ can be extracted to obtain curves that match with the experimental characteristics (Boussaada et al., 2018; Kareem & Saravan, 2018).

In Figure 5, the mathematical model of a PV panel from equation (2) is implemented in MATLAB/Simulink®, where Ic is the input signal of the controlled current source block which is calculated and expressed in equation (4), and Ig is the generated current.

$$I_c = I_{ph} - I_s\left[\exp^{(V_{pv}+R_s I_{pv})/V_T} - 1\right] \quad (4)$$

After that, a continuous voltage V_{pv} between 0 and V_{OC}, which is an open-circuit voltage, is used, as shown in Figure 6. The consequence is represented by the obtained I-V and P-V curves as it has already been illustrated in Figure 3.

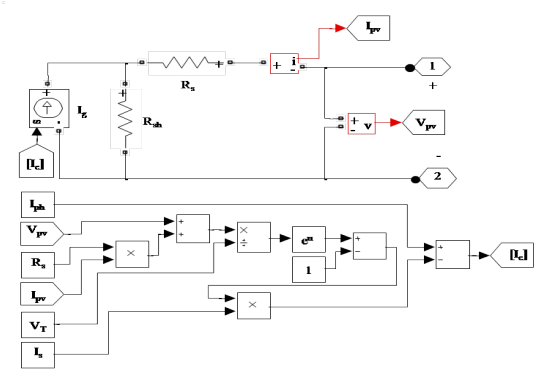

Figure 5. Simulink block diagram of PV panel model

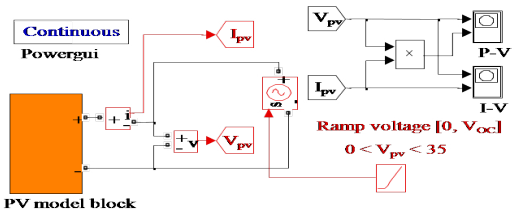

Figure 6. Simulink block diagram of PV panel characterization

2.2 DC-DC Boost Converter

In general, DC-DC converters are used to respond to two main points. The first is to ensure the adaptation of the load to the PV panel. The second point is to guarantee the optimal power transfer to the load (Abouda et al., 2013). The used converter is a DC-DC boost converter composed of switches (T, D), filter (C_{input}, L_{input}) in the input and capacitor Cout in the output. This architecture is illustrated in Figure 7.

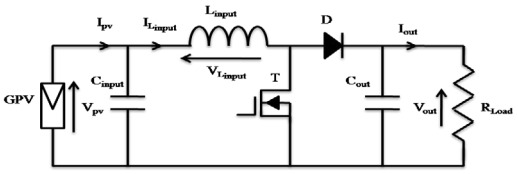

Figure 7. Boost DC-DC converter for PVS

In Figure 7, GPV is a PV source, T is a MOSFET chopper, D is a diode, and C_{input} and L_{input} are a capacitor and an inductor, respectively. The state operation of both switches leads to two phases:

➢ Phase 1: When switch T is closed and switch D is open, the input energy of the source (GPV) will be stored by capacitor C_{input} and by inductor L_{input}. The voltages across the inductor, the capacitor and the PV panel (GPV) output are at the same level:

$$V_{Linput} = V_{Cinput} = V_{pv} \quad (5)$$

The voltage across the inductor can be defined by:

$$V_{Linput} = L_{input}\frac{dI_{Linput}}{dt} \quad (6)$$

where $\frac{dI_{Linput}}{dt}$ is the inductor rate current change, dI_{Linput} is the ripple current following this inductor, and dt is the duration for which the voltage V_{Linput} is applied.

The ripple current is represented as:

$$dI_{Linput} = \frac{V_{pv}}{L_{input}}dt \quad (7)$$

➢ Phase 2: When T is open and D is closed, the stored energy will discharge in capacitor C_{out} as well as in load R_{Load}. The capacitor and the load have the same voltage. The latter is designed by output voltage V_{pv}. Then the voltage across the inductor can be shown as follows:

$$V_{Linput} = V_{Cinput} - V_{out} = V_{pv} - V_{out} \quad (8)$$

Using equation (6), the ripple current is given by:

$$dI_{Linput} = \frac{V_{pv} - V_{out}}{L_{input}} dt \quad (9)$$

The inductor current waveform is presented in Figure 8.

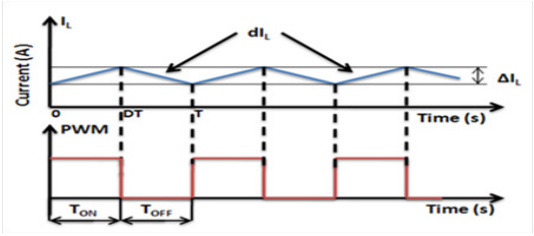

Figure 8. Current waveform and PWM

Similarly, Figure 8 depicts the PWM signal, where T is the period, T_{ON} is the on-time (phase 1), T_{OFF} is the off-time (phase 2), and D is the duty cycle defined by equation (10).

$$D = \frac{T_{ON}}{T} \quad (10)$$

It is admitted that the ripple current dI_L is related to the current difference ΔI_L flowing in inductor L as follows:

$$\Delta I_L = \int dI_L = \int \frac{V_L}{L} dt \quad (11)$$

Hence, during the on-switching cycle, the current difference flowing in inductor L_{input} is defined in equation (12):

$$(\Delta_{I_{Linput}})_{closed} = \int_0^{DT} \frac{V_{pv}}{L_{input}} dt = \frac{V_{pv} DT}{L_{input}} \quad (12)$$

Moreover, during the off-switching cycle, this current difference is defined in equation (13) as follows:

$$(\Delta_{I_{Linput}})_{opened} = -\int_{DT}^{T} \frac{V_{pv} - V_{out}}{L_{input}} dt = \frac{-(V_{pv} - V_{out})(1-D)T}{L_{input}} \quad (13)$$

In the steady-state operation, the current difference $\Delta_{I_{Linput}}$ in the inductor must be the same in the closed-circuit and opened-circuit states:

$$(\Delta_{I_{Linput}})_{closed} = (\Delta_{I_{Linput}})_{opened} \quad (14)$$

This leads to:

$$\frac{DTV_{pv}}{L_{input}} = \frac{-(1-D)(V_{pv} - V_{out})T}{L_{input}} \quad (15)$$

The ratio output/input voltage is regulated by adjusting the ratio of the on/off time in the PWM signal. It is given by:

$$\frac{V_{out}}{V_{pv}} = \frac{1}{1-D} \quad (16)$$

2.3 Controller Design Process

The main task of the design controller is to track the MPP provided by the PVS for any user load under varying climatic conditions. This technique is guaranteed by two parts: hardware and software, where an Arduino Uno® board is used to capture the PV panel current and voltage (I_{pv}, V_{pv}) and generate a PWM signal. PC software is used to turn and monitor the algorithm, while an order is given to the Arduino Uno® board to generate the PWM signal and adjust the available duty cycle. Furthermore, the duty cycle can be continuously given from 0 to 1 and can show the PV panel characteristic curves.

2.3.1 Proposed Algorithm

The suggested algorithm searches for the duty cycle required to reach the MPP of the PV source. The present approach is based on the impedance matching between the source impedance (CIPV) and the load impedance, at MP transfer.

At maximum power, P_{pv} is in its optimal power (Sengar, 2014):

$$\frac{dP_{pv}}{d_t} = V_{pv} \frac{dI_{pv}}{d_t} + I_{pv} \frac{dV_{pv}}{d_t} = 0 \quad (17)$$

Otherwise (Routray et al., 2021):

$$\frac{dP_{pv}}{dI_{pv}} = V_{pv} + I_{pv} \frac{dV_{pv}}{dI_{pv}} = 0 \quad (18)$$

According to the voltage-current (V-I) characteristic, the slope $\frac{dV_{pv}}{dI_{pv}}$ is negative at any point in the V-I curves of the PV sources. Indeed, if voltage V_{pv} increases, current I_{pv} decreases, and vice versa, as depicted in Figure 9.

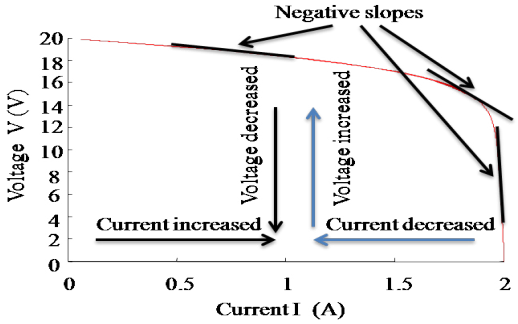

Figure 9. Trace of slope in V-I curve

Z denotes the instantaneous impedance as:

$$Z = -\frac{dV_{pv}}{dI_{pv}} \tag{19}$$

By substituting equation (19) into equation (18), one obtains:

$$V_{pv} - ZI_{pv} = 0 \tag{20}$$

V_Z denotes the instantaneous potential of the Z impedance, and it is calculated as follows:

$$V_Z = ZI_{pv} \tag{21}$$

By substituting equation (21) into equation (20), one obtains:

$$V_{pv} - V_Z = 0 \tag{22}$$

Consequently, at maximum power:

$$V_{pv} = V_Z \tag{23}$$

Thus, in this technique, the instantaneous voltage V_Z will be compared to the potential output voltage V_{pv}, as shown in the control flowchart algorithm in Figure 10.

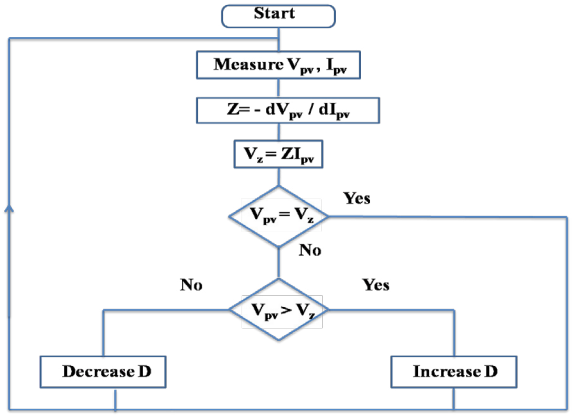

Figure 10. Flowchart of proposed algorithm

Therefore, when equation (23) is fulfilled, the PVS is in a matched system and the PV source reaches its maximum output power. Comparing V_{pv} to V_Z, the D duty cycle increment or decrement follows the decision of the algorithm of the flowchart. Afterwards, V_{pv} and I_{pv} are measured. This process is repeated until V_Z and V_{pv} become equal. Thus, the power will rapidly converge to the optimum power and the MPP will be reached, as depicted in Figure 11.

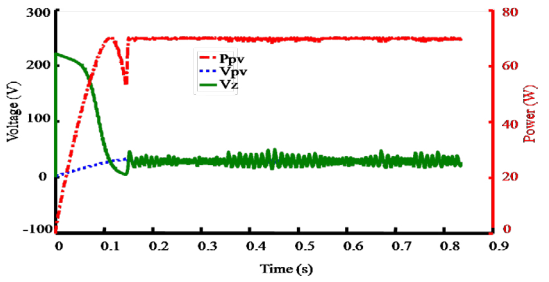

Figure 11. Dynamic responses of output power and voltage during MPPT in simulation tools

2.3.2 Arduino Uno® Board

The Arduino Uno® board is an open-source microcontroller family of electronic cards. These cards are based on a simple input/output interface and a development environment close to the C language. The Arduino Uno® board is the first stable version of the Arduino board. Arduino can generate only a numeric signal voltage to feed the gate terminal of the MOSFET.

2.3.3 Implementation

V_{pv} and I_{pv} are acquired by an Arduino Uno® board using a MATLAB/Simulink® interface, as given in Figure 12.

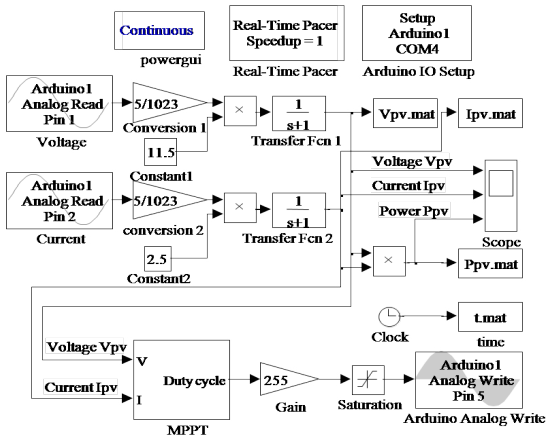

Figure 12. MATLAB/Simulink® interface

The proposed algorithm is also implemented in MATLAB/Simulink®, as shown in Figure 13. The duty cycle is calculated and sent to Arduino with the use of MATLAB/Stateflow®, which will increment or decrement these ones with a changeable step, as presented in Figure 14.

Stateflow® is a graphical language applied in MATLAB/Simulink®, and it models and simulates the logic decision flowchart including states and transitions (Ahmed et al., 2013). In this case, a

flowchart, as given in Figure 14, is suggested to increment or decrement a variable (n) (duty cycle) with a chosen step (0.001, 0.002 or 0.0008). In Figure 14, (r) represents the logical transition. When it is equal to 1, the variable (n) will increase with a specific step. Otherwise, this variable will decrease with a specific step. This leads to an increase in the speed of the convergence rate and a decrease in the amplitude of oscillations around the MPP.

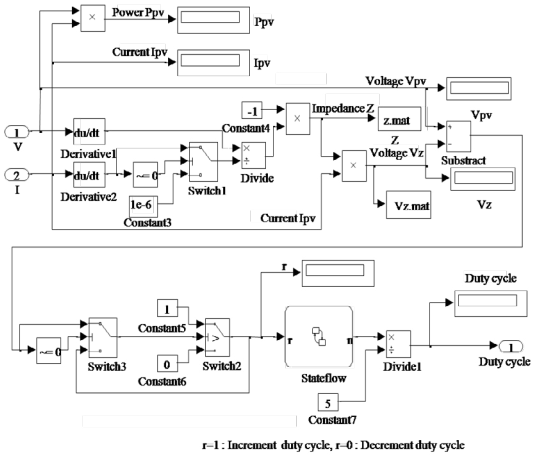

Figure 13. MATLAB/Simulink® block diagram of proposed algorithm

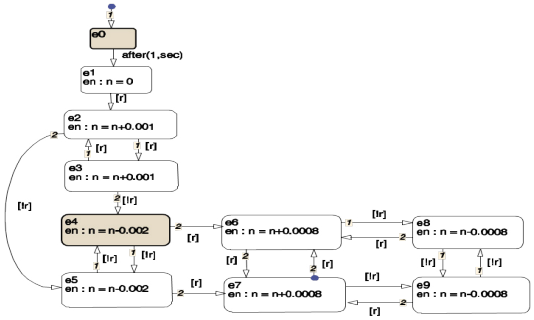

Figure 14. MATLAB/Stateflow® block diagram

3. Simulation Results

By using MATLAB/Simulink®, the present work stimulates the proposed PVS so that PV characteristic curves can be obtained and the MPPT convergence can be noticed.

3.1 Characterization

To obtain the I-V and P-V characteristic curves, as shown in Figure 15, a higher-level load is connected to the boost converter (as it has been previously illustrated in Figure 7), in order to obtain an open circuit V_{OC} in the zero-duty cycle, because in the zero-duty cycle the PV panel is connected directly to the load. The sweep of all points between the open-circuit and short-circuit states is guaranteed, while varying the duty cycle between [0, 1]. Stateflow® will continuously increase the duty cycle between [0, 1].

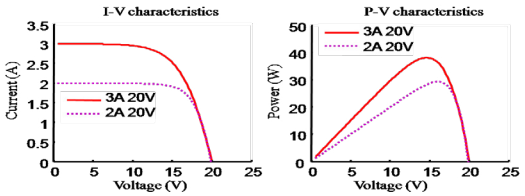

Figure 15. PV panel characteristic

3.2 MPPT

In this situation, Stateflow® receives the order to increment or decrement the duty cycle. Finally, the available duty cycle will be adjusted to converge the PVS in MPPT, and the V_{pv}, I_{pv} and P_{pv} values will converge to their optimum, as illustrated in Figures 16, 17, and 18. This process is simulated with different values of load (1000Ω, 300Ω and 30Ω) and is manipulated for two climatic conditions (ISC=3A, VOC=20V and ISC=2A, VOC=20V). It is remarked that for the different load values, the suggested algorithm converges the PVS with the same optimal values of each climatic conditions (characteristic curve), so the PV power depends on the load level and the climatic conditions and ensures the uniqueness of the optimal load impedance for the MPPT of the exploited PV sources.

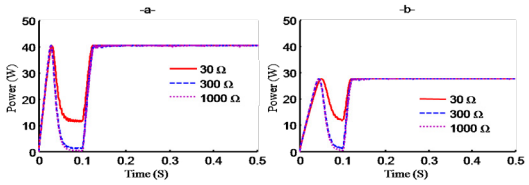

Figure 16. Output power P_{pv} at MPPT
a) I_{SC}=3A, V_{OC}=20V; b) I_{SC}=2A, V_{OC}=20V

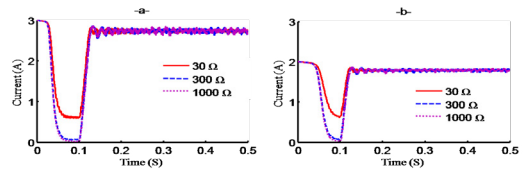

Figure 17. Output current I_{pv} at MPPT
a) I_{SC}=3A, V_{OC}=20V; b) I_{SC}=2A, V_{OC}=20V

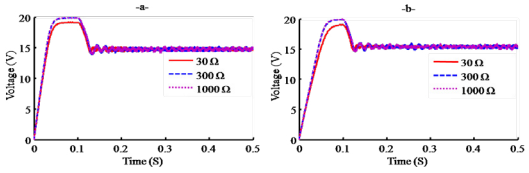

Figure 18. Output voltage V_{pv} at MPPT
a) I_{SC}=3A, V_{OC}=20V; b) I_{SC}=2A, V_{OC}=20V

3.3 Varying Irradiation

Starting with 500 W/m² (I_{SC}=2A; V_{OC}=20V; P_{opt}=30W) and increasing to 750 W/m² (ISC=3A; V_{OC}=20V; P_{opt}=40W) after 2 seconds, the proposed method can track the MPP with efficient results, without any deviation, as illustrated in Figures 19, 20 and 21.

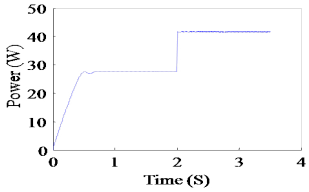

Figure 19. Simulation output power P_{pv} at MPPT of sudden climate change

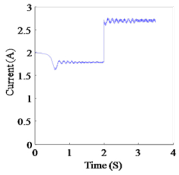

Figure 20. Simulation output current I_{pv} at MPPT of sudden climate change

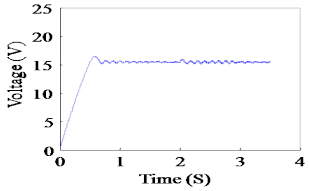

Figure 21. Simulation output voltage V_{pv} at MPPT of sudden climate change

4. Experimentation Results

The experimental setup proposed in the present paper is employed to evaluate the performance of this technique. The objective is to track the optimal power. Furthermore, the PV panel characteristic curves can be obtained. The proposed MPPT algorithm is implemented, as it has been previously illustrated in Figures 12, 13 and 14.

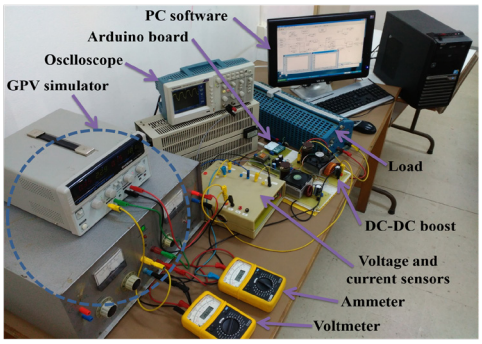

Figure 22. Experimental set-up

The experimental setup bench is shown in Figure 22. This bench consists of PC software, an Arduino Uno® board, a DC/DC boost converter, and two sensors used to acquire current I_{pv} and voltage V_{pv} of a GPV simulator (Boussaada et al., 2019).

4.1 Characterization

In the first state of this experiment, the PV panel is characterized using a DC/DC converter method. A DC/DC boost converter is connected to a higher-level load. The Arduino Uno® board and the PC software are used to scan all the points between the open circuit V_{OC} and the short circuit I_{SC}. These can provide the I-V and P-V characteristic curves, as depicted in Figure 23.

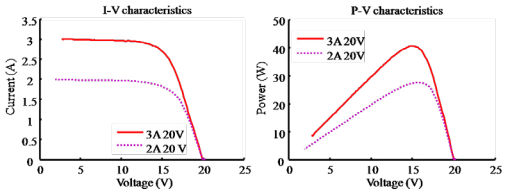

Figure 23. GPV characteristics under different conditions: I_{SC}=3A, V_{OC}=20V and I_{SC}=2A, V_{OC}=20V

4.2 MPPT

In the second state of this experiment, the MPPT of the PVS can be obtained in the two cases of climatic conditions and for the same different values of load R_{Load}, as shown in Figures 24, 25 and 26.

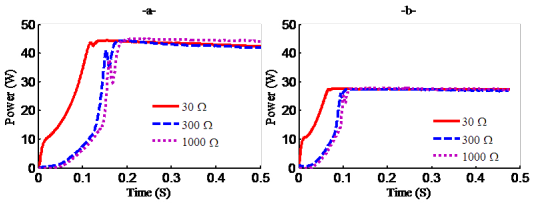

Figure 24. Output power P_{pv} at MPPT
a) I_{SC}=3, V_{OC}=20V; b) I_{SC}=2A, V_{OC}=20V

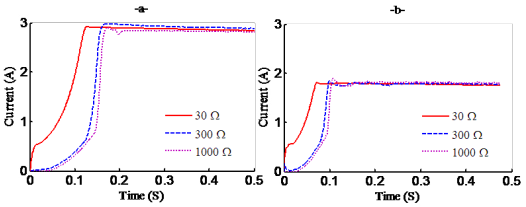

Figure 25. Output current I_{pv} at MPPT
a) I_{SC}=3, V_{OC}=20V; b) I_{SC}=2A, V_{OC}=20V

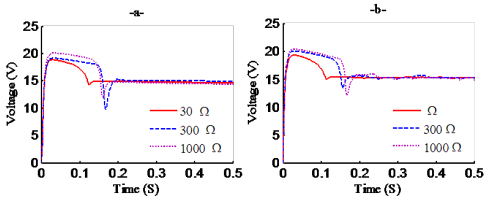

Figure 26. Output voltage I_{pv} at MPPT
a) I_{SC}=3, V_{OC}=20V; b) I_{SC}=2A, V_{OC}=20V

The proposed MPPT algorithm is used to force the PV source (panel, GPV) to operate in its

optimal point, and it gives the same MPP for the different load values, according to the climatic conditions. Figures 24, 25 and 26 represent the output response of the optimal values of power P_{pv}, current I_{pv} and voltage V_{pv}. Under these conditions (climatic conditions and load variations), the PVS converges at the operating point of each condition and with the same optimal values in different variation R_{Load} load values.

4.3 Varying Irradiation

In the experimental case, the MPPT is reached according to a certain climate change (starting with 500 W/m^2 and increasing to 750 W/m^2 after 2 seconds). The result is in good agreement with simulation, as shown in Figures 27, 28, and 29.

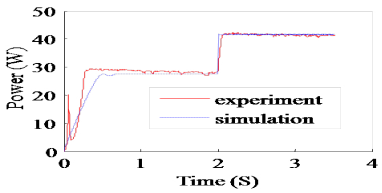

Figure 27. Output power P_{pv} at MPPT of sudden climate change

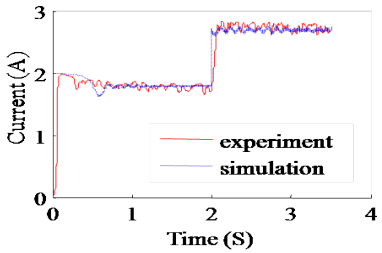

Figure 28. Output current I_{pv} at MPPT of sudden climate change

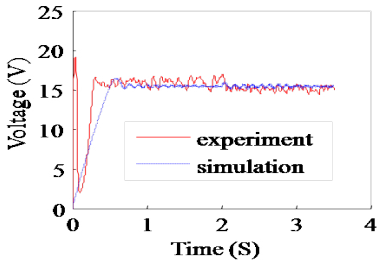

Figure 29. Output voltage V_{pv} at MPPT of sudden climate change

5. Conclusion

In this paper, a new MPPT method based on CIPV matching has been put forward. The main benefit of the suggested method is the PVS self-adjustment in all times at an available MP, with accurate and adaptive tracking performance. In addition, the incremental or decremental duty cycle with a variable step-size provides a rapid and precise convergence to the MPP.

The other objective has been to obtain the I-V and P-V characteristic curves with a modification in the implementation of the flowchart algorithm. The proposed MPPT algorithm has been implemented in a MATLAB/Simulink® environment using a DC-DC boost converter. The algorithm is simple in structure and can be easily implemented. The changing incremental or decremental step size of the duty cycle is obtained with the suggested algorithm in combination with the Stateflow® event. The proposed controller can also follow the varying irradiances and allow the PVS to achieve MP during its entire operation.

In the experimental set-up, the I-V and P-V characteristics of the GPV have been generated. Then, MPPT has been obtained with high efficiency. Comparing the optimum power observed in the P-V characteristic to that obtained by the developed algorithm, it can be concluded that the same results have been obtained. In fact, these experimental results have been as good as the simulation ones. Finally, the effectiveness of the proposed method has been observed in state condition. In addition, there is no deviation from the MPP under various weather conditions. As a future work perspective, the modality in which these methods react under shaded weather conditions will be studied.

REFERENCES

Abouda, S., Nollet, F., Essounbouli, N., Chaari, A. & Koubaa, Y. (2013) Design, Simulation and Voltage Control of Standalone Photovoltaic System Based MPPT: Application to a Pumping system. *International Journal of Renewable Energy Research*. 3(3), 538-549. doi: /doi.org/10.20508/ijrer.v3i3.712.g6176.

Ahmed, R., Namaane, A. & M'Sirdi, N. K. (2013) Improvement in perturb and observe method using state flow approach. *Energy Procedia*. 42, 614-623. doi: 10.1016/j.egypro.2013.11.063.

Alshareef, M. (2021) An Improved MPPT Method Based on Fuzzy Logic Controller for a PV System. *Studies in Informatics and Control*. 30(1), 89-98. doi: 10.24846/v30i1y202108.

Anani, N. & Ibrahim, H. (2020) Performance Evaluation of Analytical Methods for Parameters Extraction of Photovoltaic Generators. *Energies*. 13(18), p. 4825. doi: 10.3390/en13184825.

Boussaada, M., Abdelati, R. & Yahia, H. (2018) Emulation, model identification and new-approach characterization of a PV panel. *International Journal of Engineering, Transactions B: Applications*. 31(8), 1222-1227. doi: 10.5829/ije.2018.31.08b.09.

Boussaada, M., Abdelati, R. & Yahia, H. (2019) Emulating and amplifying an I-V panel based on an electrical model of a PV cell. In: *10th International Renewable Energy Congress (IREC), 26-28 March 2019, Sousse, Tunisia*. pp. 1-6. doi: 10.1109/IREC.2019.8754554.

Boutabba, T., Drid, S., Chrifi-Alaoui, L. & Benbouzid, M. E. (2018) A new implementation of maximum power point tracking based on fuzzy logic algorithm for solar photovoltaic system. *International Journal of Engineering, Transactions A: Basics*. 31(4), 580-587. doi: 10.5829/ije.2018.31.04a.09.

Brito, E. M. D. S., Antônio, A. D. S., Cupertino, A. F. & Pereira, H. A. (2014) Characterization of solar panel using capacitive load. In: *11th IEEE/IAS International Conference on Industry Applications, 7-10 December 2014, Juiz de Fora, Brazil*. pp. 1-7. doi: 10.1109/INDUSCON.2014.7059472.

Chellal, M., Guimaraes, T. F. & Leite, V. (2021) Experimental Evaluation of MPPT algorithms: A Comparative Study. *International Journal of Renewable Energy Research (IJRER)*. 11(1), 486-494. doi: 10.20508/ijrer.v11i1.11797.g8164.

Fares, M. A., Atik, L., Bachir, G. & Aillerie, M. (2017) Photovoltaic panels characterization and experimental testing. *Energy Procedia*. 119, 945-952. doi: 10.1016/j.egypro.2017.07.127.

Haihong, B., Weiping, Z. & Bing, C. (2016) Control simulation and experimental verification of maximum power point tracking based on RT-LAB. *International Journal of Engineering, Transactions A: Basics*. 29(10), 1372-1379. doi: 10.5829/idosi.ije.2016.29.10a.07.

Husain, M. A., Tariq, A., Hameed, S., Arif, M. S. B. & Jain, A. (2017) Comparative assessment of maximum power point tracking procedures for photovoltaic systems. *Green Energy and Environment*. 2(1), 5-17. doi: 10.1016/j.gee.2016.11.001.

Ibnelouad, A., Kari, A. E. L., Ayad, H. & Mjahed, M. (2021) Multilayer artificial approach for estimating optimal solar PV system power using the MPPT technique. *Studies in Informatics and Control*. 30(4), 109-120. doi: 10.24846/v30i4y202110.

Jana, J., Samanta, H., Bhattacharya, K. D. & Saha, H. (2016) A four stage battery charge controller working on a novel maximum power point tracking based algorithm for solar PV system. In: *21st Century Energy Needs-Materials, Systems and Applications (ICTFCN), 17-19 November 2016, Kharagpur, India*. pp. 1-4. doi: 10.1109/ICTFCEN.2016.8052702.

Kanth, B. S., Sainath, C. V. S. & Sandeep, G. (2015) PV Fed Modified SEPIC Converter. *International Journal of Scientific & Engineering Research*. 6(3), 542-551.

Kareem, M. S. A. & Saravan, M. (2018) A novel modeling approach to predict the output performance of photovoltaic modules under different environmental condition. *Simulation*. 94(10), 861-872. doi: 10.1177/0037549718761208.

Khatib, T., Elmenreich, W. & Mohamed, A. (2017) Simplified I-V characteristic tester for photovoltaic modules using a DC-DC boost converter. *Sustainability*. 9(4), 657. doi:10.3390/su9040657.

Remy, G., Bethoux, O., Marchand, C. & Dogan, H. (2009) *Review of MPPT Techniques for Photovoltaic Systems*. Laboratoire de Génie Electrique de Paris (LGEP)/SPEE-Labs, Université Pierre et Marie Curie. p. 6.

Routray, D., Rout, P. K. & Sahu, B. K. (2021) A brief review and comparative analysis of two classical MPPT techniques. In: *International Conference in Advances in Power, Signal, and Information Technology (APSIT), 08-10 October 2021, Bhubaneswar, India*. pp. 1-6. doi: 10.1109/APSIT52773.2021.9641301.

Salih, Y. S. M., Jabur, K. H. & Kadhim, L. A. (2016) Analysis of temperature effect on a crystalline silicon photovoltaic module performance. *International Journal of Engineering, Transactions B: Applications*. 29(5), 722-727. doi: 10.5829/idosi.ije.2016.29.05b.17.

Sengar, S. (2014) Maximum power point tracking algorithms for photovoltaic system: A review. *International Review of Applied Engineering Research*. 4(2), 147-154. doi: 10.1016/j.rser.2015.12.105.

Senthilkumar, S., Mohan, V., Mangaiyarkarasi, S. P., & Karthikeyan, M. (2022) Analysis of single-diode PV model and optimized MPPT model for different environmental conditions. *International Transactions on Electrical Energy Systems*. pp. 17. doi: 10.1155/2022/4980843.

Sruthy, T. S. & Mohan, F. (2017) Fast-converging MPPT technique for photovoltaic system using dsPIC controller. In: *11th International Conference on Intelligent Systems and Control (ISCO), 05-06 January 2017, Coimbatore, India.* pp. 140-144. doi: 10.1109/ISCO.2017.7855969.

Yadav, A. P. K., Thirumaliah, S. & Haritha, G. (2012) Comparison of MPPT algorithms for DC-DC converters based PV systems. *International Journal of Advanced Research in Electrical, Electronics and Instrumentation Engineering*. 1(1), 18-23.

Zhou, Z. & Macaulay, J. (2017) An Emulated PV Source Based on an Unilluminated Solar Panel and DC Power Supply. *Energies*. 10(12), 2075. doi:10.3390/en10122075.